JOURNAL OF MATERIALS SCIENCE 19 (1984) 2039–2056

Stress–orientation–strain relationships in non-crystalline polymers

Part 3 *Towards a description of glassy deformation*

D. J. BROWN, A. H. WINDLE
Department of Metallurgy and Materials Science, University of Cambridge, Cambridge, UK

The two-mode deformation model developed in Part 2 of this series of papers [1] is modified by the application of different rate dependences to the two components, in order to extend its scope into the vicinity of the glass transition and below. The modified treatment predicts the characteristic change in shape of the stress–strain curve near T_g. It also accounts for the observed trends in orientation–strain behaviour, predicting that orientation as measured by $\langle P_2(\cos\phi)\rangle$ develops more rapidly as rate effects become more significant, while $\langle P_4(\cos\phi)\rangle$ remains very small. The differing recovery behaviour of orientation and strain on annealing is successfully accounted for, and the application of the model to annealing data for atactic PMMA allows the relative magnitude of the two rate constants to be determined for this material. In the adaptation of the model to glassy deformation, the number of variables is kept to a minimum, with only a single adjustable parameter applied to each mode in order to limit the deformation rate.

1. The time factor in deformation

The model discussed in Part 2 of this series of papers [1], to which we shall now refer for brevity as the "fast model", ignores the effect of time on deformation processes. This is reasonable for deformation above the glass transition, where the molecular structure of the rubber is in equilibrium under the applied stress, but modification is needed before deformation at lower temperatures can be considered. We then have to consider deformation as being governed by some sort of rate process, so that the effect of time or of strain rate will become important. As a first and simplest approximation we treat the "rubber-like" behaviour as a limiting case to which our "glassy" behaviour will tend at long times or low strain rates.

1.1. Incorporation of time in the model

We will approach the question of the time factor by first considering some simple features of elementary rate theory. Suppose we have a system in which some entity can occupy one of two states, A and B, which have equal energy in the absence of any external interference (e.g. that due to the application of a stress). Suppose further that the transition from state A to state B, or vice versa, involves the surmounting of an energy barrier of height ΔE.

This situation is illustrated in Fig. 1a; the rate of transition from A to B will match the rate from B to A and will be given by

$$\text{Rate} \sim nf\exp(-\Delta E/kT) \qquad (1)$$

where n is the number of entities available and f is some vibration frequency.

An applied stress will have the effect of biasing the energy barrier (Fig. 1b). Let the stress be σ, the "cross-sectional area per entity" perpendicular to the direction of σ be a, and the displacement (parallel to σ) per transition be l. The entity concerned only has to move a distance $l/2$ before it reaches the "top" of the "activation hump": and it will then move immediately "down" into the next equilibrium position. We therefore write the "bias energy" as $\sigma al/2$. The "forward" rate (A to B) will then be given by

0022–2461/84 $03.00 + .12

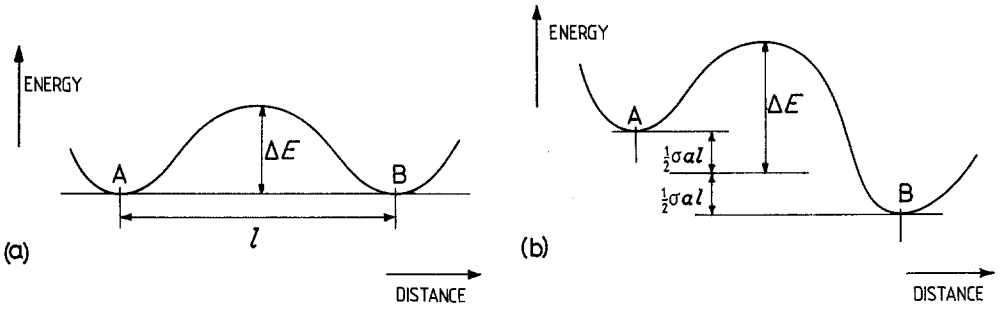

Figure 1 Rate processes: schematic energy barrier. (a) Symmetrical, (b) stress-biased, σ = stress, l = displacement, a = cross-sectional area per entity.

$$\text{Rate A} \rightarrow \text{B} \sim nf \exp -[(\Delta E - \sigma al/2)/kT]$$

and the "backward" rate (B to A) by

$$\text{Rate B} \rightarrow \text{A} \sim nf \exp -[(\Delta E + \sigma al/2)/kT]$$

so that we have a finite net rate in the A → B direction,

$$\begin{aligned}\text{Net rate} \sim\ & nf \exp(-\Delta E/kT)[\exp(\sigma al/2kT) \\ & - \exp(-\sigma al/2kT)] \\ =\ & nf \exp(-\Delta E/kT) \\ & \times 2 \sinh(\sigma al/2kT) \qquad (2)\end{aligned}$$

where the "backward" rate can be neglected at high rates of strain.

Such is the fundamental idea behind activated flow processes; the approach leads to the theory of viscosity first set out in detail by Eyring [2]. We do not exactly want a straightforward viscous flow situation; it leads to infinite flow as time tends to infinity or as strain rate tends to zero. Instead, we require the long-time limit to be equivalent to the "fast" model of Part 2 [1]. Nevertheless, the idea of an activated process is a useful one.

The simplest approach we can take to begin developing a treatment of glassy deformation is to apply a time dependence, in the form of a rate constant, to one or both deformation modes. There is no reason to suppose that the two modes will be equally affected, at a given temperature and strain rate, by time dependence. It is not suggested that the deformation behaviour of real polymer glasses can be fully described by this procedure involving only one or two simple rate constants. The procedure is to be seen as a means of introducing time dependence independently into each component of the two-mode model with the minimum increase either in mathematical complexity or in the number of adjustable parameters. We may then examine the extent, if any, to which the modified model is capable of describing the observed behaviour.

1.2. Choice of rate constants

The two-component approach, as outlined in Part 1 [3], implies that the extensional mode will be the longer-range of the two deformation modes, in that we may think of a unit moving "bodily" through distances comparable to its length. We have, in contrast to the proposed orientational mode, a shift of the centre of gravity of the unit. It is therefore reasonable to apply a "time factor" or strain rate effect first to the extensional mode, and to examine the effect of doing so on the behaviour predicted by the model. Subsequently we can apply a time factor also to the orientational mode.

1.3. Computation method

The calculation of strain and orientation for the model developed in Part 2 [1] is performed by a straightforward set of computer programs written in Fortran. The method is based upon successive equal increments of the true stress parameter q, typically with an increment size $\Delta q = 0.1$. The model is thus one which imposes a constant rate of change of true stress.

This fact may safely be ignored in modelling rubber-like behaviour. As soon as we move towards T_g, however, it becomes most important to distinguish between deformation at constant strain rate and deformation at constant "stress rate". It is apparent from mechanical testing that the behaviour of a glassy polymer will differ considerably from one type of loading to the other. Furthermore, in a simple uniaxial tensile test, the difference between constancy of true stress and

strain, and constancy of their nominal analogues, will be important.

For modelling purposes it is most useful to treat the case of deformation at some specified constant nominal strain rate, since most experimental data are obtained under this condition. At each step of the computation it is then necessary to calculate the strain rate, compare the result with the specified rate, and if necessary repeat the step with an amended value either of the true stress parameter increment Δq, or of the time increment Δt. It has proved more convenient in practice to amend Δt and to repeat the calculations for each step of the computation, using an iterative technique to arrive at the specified strain rate (within a tolerance of typically 3%) before proceeding to the next computation step.

2. Extensional component

Our earlier consideration of the extensional component of strain λ_e immediately suggests a process we can try activating – the removal of a unit from, or the addition of one to, those which intersect our "sampling plane". The "forward" process will then be that which encourages strain in the direction required by the applied stress. This, following the approach in Part 2 [1], will be the removal of a unit.

We assume first that the term al in Equation 2 can be taken as equivalent to the "volume per ellipsoidal unit" v. Suppose that the number of units available for "removal" is N_1 and that the number available for "addition" is N_2. From Equation 2 the net rate of change of N will be given by:

$$\text{Rate} = N_1 f \exp(-\Delta E/kT) \exp(q/2) - N_2 f \exp(-\Delta E/kT) \exp(-q/2) \quad (3)$$

making the substitution $q = \sigma v/\alpha kT$ again. At equilibrium the net rate of change of N must be zero, so:

$$\frac{N_2}{N_1} = \frac{\exp(-q/2)}{\exp(q/2)} = \exp(-q) \quad (4)$$

This should be equivalent to the situation given by Equation 17 of Part 2, which would give:

$$\frac{N-N^*}{N_0-N^*} = \exp(-q) \quad (5)$$

Comparison of these two expressions suggests that we make the associations

$$N_1 = N - N^* \quad (6)$$

$$N_2 = N_0 - N^* \quad (7)$$

so that the net rate of change of N will now be

$$\text{Rate} = f\exp(-\Delta E/kT)[(N-N^*)\exp(q/2) - (N_0-N^*)\exp(-q/2)] \quad (8)$$

Consider now one particular step in the deformation, comprising an increment of stress (bringing the value of our "true stress parameter" to q) followed by an interval of time Δt. Let the value of (N/N_0) at the beginning of the interval be (N_p/N_0). Then we have:

$$\frac{N}{N_0} = \frac{N_p}{N_0} - \left[\left(\frac{N}{N_0} - \frac{N^*}{N_0}\right)\exp(q/2) - \left(1 - \frac{N^*}{N_0}\right)\exp(-q/2)\right] F \quad (9)$$

abbreviating $F = f\exp(-\Delta E/kT)\,\Delta t$. $(N/N_0)_p$ is simply given by the reciprocal of the previous value of λ_e from the preceding "step", and is easily incorporated in the computation. Rearranging, we obtain:

$$\frac{N_0}{N} = \frac{1 + F\exp(q/2)}{\frac{N_p}{N_0} + \left[\frac{N^*}{N_0}\exp(q/2) + \left(1 - \frac{N^*}{N_0}\right)\exp(-q/2)\right] F} \quad (10)$$

It is useful to define

$$C_e = F/\Delta t$$

(so that we can later give different strain rate dependences to the orientational component of strain λ_0 and the extensional component λ_e). The extensional variables are now:

$$K = N_0/N^* \quad (11)$$

$$C_e = f\exp(\Delta E/kT) \quad (12)$$

and as before, λ_e is given by the reciprocal of Equation 10:

$$\lambda_e = N/N_0$$

which approaches the fast model as C_e tends towards infinity.

2.1. Severity of the rate effect

The "time factor" will affect a rate process more strongly if the imposed strain rate is increased,

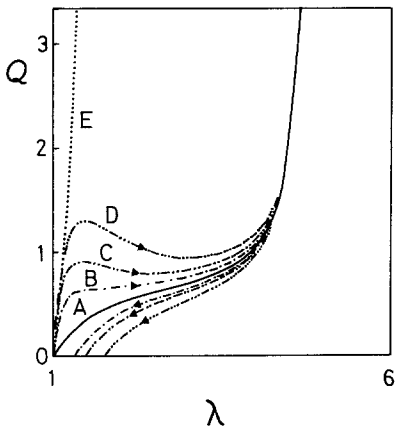

Figure 2 Nominal stress–strain curves for aspect ratio 3, $K = 3$, showing strain rate dependence when a rate constant is applied to the extensional deformation mode. Arrows indicate loading and unloading curves. (A) fast model; (B) rate $\propto 1$ (computation: $C_e = 0.2$, $\Delta\lambda/\Delta t = 0.1$); (C) rate $\propto 2$ ($C_e = 0.1$, $\Delta\lambda/\Delta t = 0.1$); (D) rate $\propto 4$ ($C_e = 0.05$, $\Delta\lambda/\Delta t = 0.1$); (E) orientational mode only (for infinite strain rate).

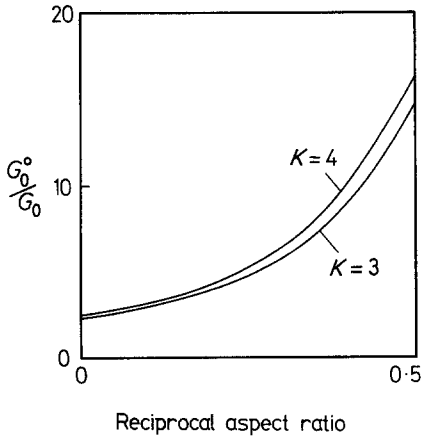

Figure 3 The effect of "freezing out" the extensional mode: G_0 = initial slope of Q against λ curve (= initial modulus in units of q) for fast model; G_0^o = initial slope when orientational mode only is operative. The behaviour is sensitive to aspect ratio, but not significantly to fractional constraint on extensional mode.

the temperature reduced, or the "activation barrier" raised. While the latter is to be seen as basically a material property, it may not be sufficient to regard it as constant over all experimental conditions. It is common to view ln(strain rate) as having an inverse effect to absolute temperature (to a first approximation). In order to examine in a general way the effect of introducing time dependence into the model, we shall refer to the "severity" of the rate effect, which will encompass all three factors. Variation in severity can then most conveniently be modelled by changing the value of C_e.

3. Effect of rate dependence on extensional mode

To investigate the effect of the time factor we take the fast model with the parameters previously chosen, i.e. aspect ratio 3, $K = 3$, and apply a rate constant to the extensional mode as described by Equation 10. As we are affecting only one mode, it is immaterial at this stage whether we alter the parameter F in Equation 10 by changing the value of the rate constant (effectively C_e) or the strain rate $\Delta\lambda/\Delta t$.

The effect on the nominal stress–strain curve of varying F is shown in Fig. 2. For the purposes of computation, $\Delta\lambda/\Delta t$ has been fixed at 0.1 and C_e given the values 0.2, 0.1, 0.05; this is of course equivalent to assuming a fixed C_e, characteristic of the material at a given temperature, and varying the imposed strain rate by successive factors of 2. Curve A shows the original fast model: this would correspond to $C_e = 0$ or to an infinitely slow strain rate. Two features are apparent. Firstly the inflexion in the curve becomes much more pronounced, and for a sufficiently severe rate effect, the nominal stress reaches a maximum and then falls to a minimum as the limiting strain is approached. Such a fall would correspond to a case of geometrical softening: we are, of course, imposing a continually increasing q, and the true stress σ will therefore also be continually increasing ($q = v\sigma/kT$), provided that the volume v per unit remains constant.

The second feature is the greatly increased initial modulus. We recall that the initial modulus is a property which affords one of the most drastic contrasts between the rubbery and glassy states, differing by as much as three orders of magnitude. As the strain rate becomes large, the extensional component of the model will become entirely "frozen out" within the time-scale of the hypothetical test which is being modelled (Curve E): the limiting modulus will then be that associated with the orientational mode alone. This makes a difference of about a factor of 7, compared to the fast model, for an aspect ratio of 3 and $K = 3$: Fig. 3 shows the difference as a function of

aspect ratio*. Freezing the extensional mode alone therefore would not appear to produce such a dramatic increase in initial modulus as would be expected on going fully into the glassy regime, particularly when we consider in more detail the factors which contribute to deformation in the initial steep part of the glassy stress–strain curve. It should also be noted that the conversion from q to stress (i.e. D_{q0} to G_0) is dependent on the temperature T and the volume v per unit: the change in absolute temperature associated with the introduction of a time factor will make only a relatively small difference to the initial modulus G_0, a reduction in temperature leading to a reduction in G_0 for a given calculated D_{q0}. There is, however, a possibility of a change in v: as the temperature is reduced and long-range motion becomes more difficult, it might be expected that the size of entity involved in local deformation processes would change. A decrease in v would increase the resultant initial modulus G_0 for a given D_{q0} as calculated on the basis of the model.

At sufficiently high stresses the stress–strain curve approaches that of the fast model so closely as to be indistinguishable from it. The sign of Δq may then be reversed, and an "unload" curve plotted at the same nominal strain rate: such curves are also shown in Fig. 2 (reversing at $q = 20$). The area swept out between the load and unload curves increases, as we should expect, with strain rate: if the strain rate is unchanged, the unload curve reaches zero stress with the strain still finite. This could indicate that there would be little driving force for the recovery of the equilibrium state of the system, and that any tendency towards "locking" of one deformation mode by another might easily lead to permanence of deformation.

3.1. Orientation behaviour

A extensional rate constant will also affect orientation behaviour. The orientation–true stress plot will be unaffected, except via concomitant changes in temperature or v, but the orientation–strain plot will be altered as shown in Fig. 4. As for the stress–strain curve, the initial slope of the plot is increased: we then observe a pronounced levelling-off with increasing strain. This behaviour is exactly

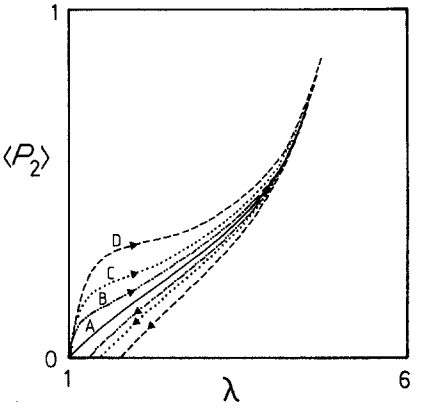

Figure 4 Orientation–strain curves for aspect ratio 3, $K = 3$, showing strain rate dependence when a rate constant is applied to the extensional deformation mode. Key as for Fig. 2.

what is observed experimentally as we move towards the glassy state. However, the plot displays a subsequent upturn to approach the fast model at high strains: this, if it is at all representative of experimental behaviour, suggests a possible problem in birefringence experiments. Given that high strains may not be experimentally accessible, the earlier part of a curve such as C in Fig. 4 might suggest an approach to an asymptotic limit corresponding to the intrinsic birefringence ($\langle P_2 \rangle = 1$). Such reasoning would then lead to the deduction of too low a value for intrinsic birefringence introduce error in the conversion from stress-optical coefficient to the differential of $\langle P_2(\cos\phi) \rangle$ with respect to stress.

4. Application of rate dependence to orientational mode alone

It is conceptually a little less easy to apply a rate constant to the orientational deformation mode, since it is less clear exactly what elementary process we can think of as being "activated", and what the associated deformation increment would be. The orientational angle ϕ can take any value from 0 to $\pi/2$, rather than a value corresponding only to one of a set of discrete energy states. Nevertheless, for the purposes of modelling we can introduce a time factor by modifying the expression for the area A of the sampling plane. At the start of a particular com-

*We note that Curve A displays a decreasing, and Curve E an increasing, gradient with increasing strain. In view of the difficulty in measuring a true initial modulus experimentally (rather than the estimated gradient over the first few per cent of strain), we might anticipate that experiment would indicate an anomalously large difference in modulus on "freezing out" the extensional mode.

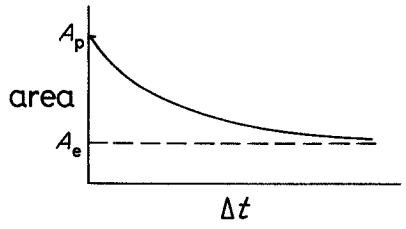

Figure 5 Area of "sampling plane" as a function of time Δt after the last stress increment Δq (schematic, with both modes subject to rate effects). A_p = area when stress was last incremented; A_e = equilibrium area for the new level of q.

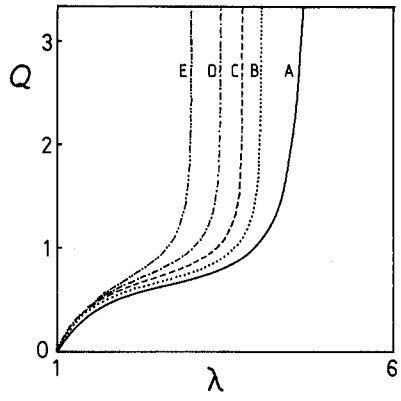

Figure 6 Nominal stress–strain curves for model with orientational mode only subject to a rate effect. Aspect ratio 3, $K = 3$. (A) fast model; (B) rate $\propto 1$ (computation: $C_0 = 0.2$, $\Delta\lambda/\Delta t = 0.1$); (C) rate $\propto 2$ ($C_0 = 0.1$, $\Delta\lambda/\Delta t = 0.1$); (D) rate $\propto 4$ ($C_0 = 0.05$, $\Delta\lambda/\Delta t = 0.1$); (E) rate infinite (or orientational mode "frozen out".

putation step let the plane area be A_p and the stress increment correspond to Δq. The equations above will then predict a new "equilibrium" area, say A_e. Let a time factor be introduced such that at the end of the computation step (time Δt).

$$A = A_e + (A_p - A_e)\exp(-C_0\Delta t) \quad (13)$$

i.e. let the area, and hence the orientational component of strain λ_0 "decay" from A_p towards A_e with a orientational rate constant C_0 (Fig. 5). The latter is closely analogous to the extensional rate constant C_e. The value of A so obtained becomes A_p for the next computation step. Clearly, if Δt is large (i.e. we impose a slow strain rate) the result of Equation 13 will tend towards the corresponding fast model result.

It is again necessary to check that the results of a calculation incorporating Equation 13 converge to a limit as the stress increment becomes small and the number of steps large, for a fixed strain rate. This limit corresponds to modelling a continuous mechanical test, performed at constant nominal strain rate. An increment $\Delta q = 0.1$ again offers a suitable compromise between accuracy and cost, though the computation is inevitably more time-consuming since the more rigorous procedure for constant strain rate modelling is employed.

4.1. Effect of orientational rate dependence on deformation

If only the orientational deformation mode is subjected to a "time factor" the stress–strain curve is affected as shown in Fig. 6. The values of C_0 used are the same as the C_e values in Fig. 2, again with $\Delta\lambda/\Delta t = 0.1$ (it should again be emphasized that altering C_0 is a computational convenience: the units of time are arbitrary and the absolute values of the rate constants unknown, so that reducing C_0 is equivalent in effect to increasing the imposed strain rate). The orientational rate constant alone has little effect on the initial slope, but increases that of the inflexion region. Not surprisingly, the trend bears little relation to the stress–strain behaviour of glasses: as has been anticipated above, we must proceed to apply rate constants to both deformation modes.

Fig. 6 indicates a progressive reduction in maximum strain from the "fast model" limit to an extension ratio equivalent to K when the orientational mode is entirely "frozen out". This behaviour follows from the constant nominal strain rate condition; the original uncorrected computation gives an unchanged maximum strain (for finite C_0) but would in effect require a time tending to infinity for its attainment.

5. Resultant behaviour: rate dependence on both modes

We now apply rate effects to both deformation modes. With increasing strain rate or smaller (i.e. more severe) rate constant, we observe firstly a more pronounced "yield" in the nominal stress-strain curve, and secondly a rapidly increasing initial modulus. These observations are true whether we keep the two rate constants the same (Fig. 7) or fix the extensional constant C_e and vary the orientational constant C_0 from infinity (equivalent to the fast model) down to $C_0 = C_e$ (Fig. 8). The latter corresponds to the gradual introduction of an orientational rate constant in addition to an extensional one.

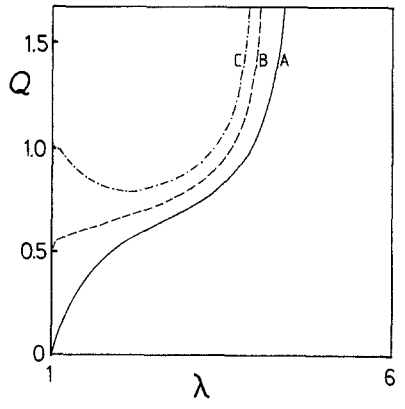

Figure 7 Nominal stress–strain curves: both modes subject to rate effects, with $C_o = C_e$. Aspect ratio 3, $K = 3$. (A) fast model; (B) rate $\propto 1$ (computation: $C_o = C_e = 0.25$, $\Delta\lambda/\Delta t = 0.1$); (C) rate $\propto 2$ ($C_o = C_e = 0.125$, $\Delta\lambda/\Delta t = 0.1$).

Of the two sets of curves shown in Figs. 7, 8, the latter will be the more appropriate to the situation envisaged in a glass, with the shorter range orientational mode less strongly affected by the time factor than the longer range extensional mode. A series of different strain rates may be modelled by taking C_e and C_o in a fixed ratio and changing $\Delta L/\Delta t$ (or equivalently fixing $\Delta L/\Delta t$ and changing C_e and C_o proportionately).

We now have to specify the fixed ratio. It will be shown below that a consideration of recovery behaviour affords one method of arriving at the appropriate ratio experimentally. For the present, however, we recall that the extensional deformation mode (the longer-range of the two) is expected to show the more severe rate dependence,

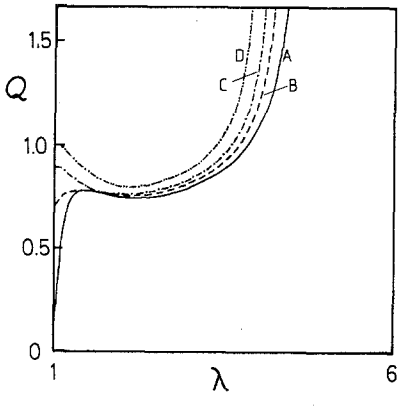

Figure 8 Nominal stress–strain curves, showing effect of gradually bringing in an orientational rate effect. Aspect ratio 3, $K = 3$, $C_e = 0.125$. (A) no orientational rate effect (C_o infinite); (B) $C_o = 0.5$; (C) $C_o = 0.25$; (D) $C_o = 0.125$.

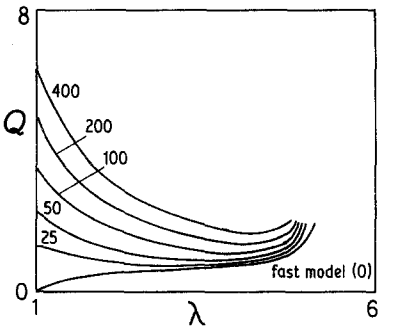

Figure 9 Nominal stress–strain curves for finite rate model: strain rate shown in arbitrary units.

and we therefore make an arbitrary choice of one order of magnitude as the ratio of the rate constants. Accordingly, we set $C_o/C_e = 10$: Fig. 9 shows a series of nominal stress–strain curves with rate constants in this ratio.

5.1. Resultant orientation behaviour

In Appendix I of Part 2 it is shown that the sampling plane area is proportional to the ratio of two integrals, I_2/I_3, where

$$I_n = \int \sec^{q+n}\psi \, d\psi$$

$$[\text{limits } 0, \arccos (1-e^2)^{1/2}]$$

where ψ is related to ϕ and the unit eccentricity e by the relation

$$\cos^2\psi = (1-e^2)/(1-e^2\sin^2\phi)$$

and the aspect ratio is equal to $(1-e^2)^{-1/2}$. Equation 13 is then equivalent to saying that the ratio I_2/I_3 decays from an instantaneous value at the start of a computation step towards the equilibrium value appropriate to the new stress level, or strictly to the new value of q.

In an analogous way we can take the expressions for $\langle\cos^{2n}\phi\rangle$ given in Appendix I of Part 2 – proportional to the ratios of similar integrals – and allow them to "decay" in a similar manner. The $\langle P_{2n}\rangle$ can then be derived. In fact we can simply "decay" the $\langle P_{2n}\rangle$ directly, since in each step we are essentially calculating changes in $\langle\cos^{2n}\rangle$ rather than absolute values. Thus:

$$\langle P_{2n}\rangle_p = \langle P_{2n}\rangle_e + (\langle P_{2n}\rangle_p - \langle P_{2n}\rangle_e) \times \exp(-C_o\Delta t) \qquad (14)$$

(subscripts have the same meaning as in Equation 13). Fig. 10 shows the predicted orientation–strain behaviour with $C_o/C_e = 10$: the structural

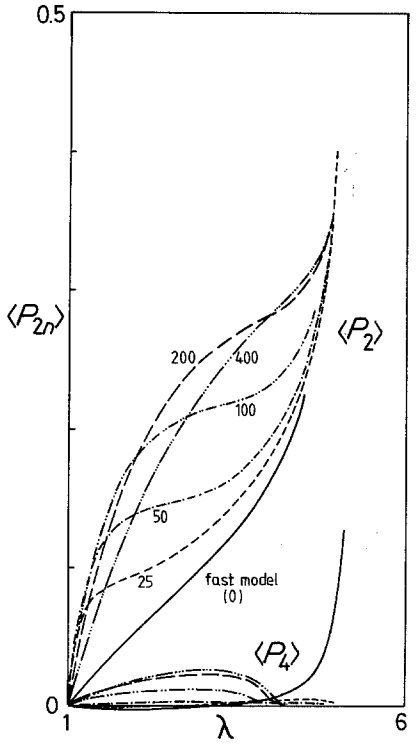

Figure 10 $\langle P_{2n}(\cos\phi) \rangle$ against ratio for finite rate model: aspect ratio 1.46, $K = 4.5$, $C_o/C_e = 10$. Number denotes strain rate (arbitrary units).

parameters are assigned the values suggested in Part 2 for PMMA. The plots correspond to the stress–strain curves of Fig. 9. The initial slope, i.e. the SNOCP, rises from the "fast model" value of 0.065 up to about 0.4, but then falls off again (for very severe rate effects, omitted from the diagram for clarity, it would fall below the "fast model" value).

The corresponding plots of orientation against q, i.e. true stress, are drawn in Fig. 11. Since no significant orientational strain develops until the threshold value of q has been attained, the plot does not "take off" until this finite q has been reached. The initial slope on doing so increases with the severity of the orientational rate effect. Additionally, the curve approaches a limiting $\langle P_2 \rangle$ which is less than 1 as time increases; this is analogous to the progressive reduction in apparent maximum strain in Fig. 6, and is again a consequence of the "constant nominal strain rate" condition. We might again anticipate problems with

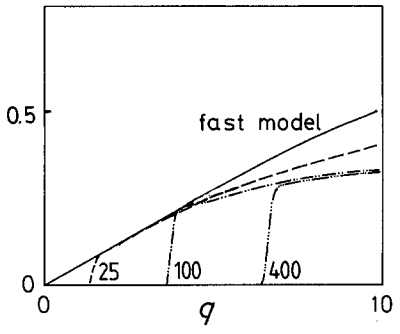

Figure 11 $\langle P_2 \rangle$ as a function of true stress parameter q. Strain rate shown in arbitrary units.

birefringence techniques: since the apparent asymptote of the plot of $\langle P_2 \rangle$ against q no longer corresponds to complete orientation, it may lead to the deduction of too low a result for intrinsic birefringence.

The magnitude of $\langle P_4 \rangle$ again remains low, as in the fast model. However, the high-strain upturn is lost: we note that even with a very gentle rate effect, which would have a barely noticeable effect on the stress–strain curve, the effect on $\langle P_4 \rangle$ at high strain is nevertheless considerable. As the rate effect becomes more severe, the uncertainty in the computed $\langle P_4 \rangle$ increases*, while at low strains $\langle P_2 \rangle$ is changing rapidly. It thus becomes more difficult (and expensive in computer time) to determine a $\langle P_4 \rangle$ against $\langle P_2 \rangle$ curve to a specified accuracy, and such a curve is therefore a less convenient means of characterizing the orientation behaviour than in the rubbery state.

We may conclude that the finite-rate model, like its "fast" counterpart, predicts $\langle P_4(\cos\phi) \rangle$ values which remain very low, and that in the finite-rate case this is true even as we approach the limiting strain. This accords with the results of most experimental techniques, with the possible exception of Raman spectroscopy: it constitutes a major difference between the predictions of the two-mode model and of the pseudo-affine deformation scheme.

5.2. Low strain behaviour and the threshold stress

Where both deformation modes are subjected to sufficiently severe rate effects (i.e. high strain rates

*The computation involves adding and dividing the results of several numerical integrations. These results are themselves small, which leads to a proportionately increasing error in $\langle P_4 \rangle$. The great expenditure of computer time which would be required in order to improve the accuracy would be unjustified in view of the considerable uncertainty associated with experimental values of $\langle P_4 \rangle$.

or small C_e, C_0) the initial portion of the stress–strain curve becomes steep, and the procedure for establishing a specified nominal strain rate fails to converge, the calculated strain rate being virtually independent of Δt^* and smaller than the rate specified. The computation procedure is designed to continue the calculation nonetheless until the specified strain rate can be attained. This is achieved, for given values of the variable parameters, at some threshold level of q (the threshold is independent of the increment Δq used in the calculation). Large increases in strain are then obtained for very little further increase in q, i.e. in true stress.

Such a large increase in strain for little increase in q is as near as we can come, in a "monotonically increasing true stress" model, to a true yield drop: it may be compared to a "soft" mechanical test, although for the uniaxial geometry the latter will usually involve a monotonically increasing nominal stress, with the exact shape of the curve depending on the elasticity and response time of the testing apparatus.

5.3. "Yielding" and the volume per unit

It is important to note that we have not introduced any qualitatively new process into the model – merely introduced a time limitation associated with each deformation mode. It is perhaps surprising, therefore, that the resulting stress–strain curve displays low-strain behaviour so reminiscent of the yielding observed experimentally.

However, if we are tentatively to associate this effect with the yielding of polymer glasses, it will be necessary to allow for a change in the scaling on the stress axis – that is, in the conversion between the dimensionless parameter q and stress, and hence in the volume per unit v. For polymers in the rubbery state, the considerations discussed in Part 2 indicate that reasonable values of v will be of order 1 nm^3†, so that at room temperature the scale factor q/σ $(= v/kT)$ will be of order 10^{-4} to 10^{-3}; i.e. the dimensionless parameter q will be numerically rather smaller than the stress in MPa.

Glassy polymers, in contrast, yield – if at all – at stresses of order 10^2 MPa. Hence, to equate the value of q associated with the "yield effect" to the yield stress of a typical glassy polymer implies a reduction in v of roughly an order of magnitude compared to the rubbery state. This would bring v down to a size comparable to that of a repeat unit (judging by the threshold values of q obtained above).

The reduction in v is not altogether implausible – we would intuitively expect deformation processes to be more localized in the glass in view of the absence of long rate mobility – but the magnitude of the reduction does seem rather drastic. Speculatively, the model is not making "yield" quite difficult enough.

6. Recoverability of the deformation

On performing a simple mechanical test at a constant strain rate, a typical polymer glass will go through a load–unload cycle which will bring it back to zero stress at some finite strain. If the specimen is subsequently allowed to recover, some further dimensional change will occur, but only at temperatures near T_g will a substantial proportion of the imposed strain recover in a measurable time. We return below to the question of differences in recovery rates of orientation and overall strain.

The constant nominal strain rate model can be used only to a limited extent to model "unloading". Fig. 2 illustrates the trend as a progressively more severe rate effect is applied to the extensional mode. When several rate effects are applied to both deformation modes, the computation ceases to be well behaved: the program calculates so great a slope in the stress–strain plot immediately after "loading" is stopped that it is unable to follow the stress–strain curve within the available computation accuracy. Extrapolation of the trend so far as we can follow it indicates that the "unload" curve, at the same strain rate (in magnitude) as for loading, will reach zero stress at a strain which increases steadily with the severity of the rate effect, and thus with decreasing temperature or increasing strain rate.

However, the model as so far developed would indicate that this residual strain will continue to recover: slowly compared to the time taken for the load–unload test itself, but nevertheless on a measurable time-scale. If we consider for simplicity only extensional strain, it is easily shown from Equation 10 (putting $q = 0$) that the extensional strain λ_e "decays" as $\exp(-C_e t)$.

*This corresponds to the situation where the strain-time plot is linear, so that $\Delta\lambda$ is proportional to Δt. $\Delta\lambda/\Delta t$ thus takes a constant value dependent on the size of increment Δq which has just been imposed.

†At 20° C the scale factor for $v = 1.0\,\text{nm}^3$ is 2.47×10^{-7}, and at 150° C it is 1.71×10^{-7}.

Thus the model as it stands will not predict the effectively permanent, plastic deformation of polymer glasses. This can be understood in terms of the procedure we have used to introduce rate dependence into the two-mode model. Our two simple exponential terms, with rate constants C_0 and C_e, will clearly be inadequate for a full description of the behaviour of real glasses: such a description requires a more complex analysis of the relationship between stress, time and temperature, involving additional parameters such as are incorporated in the Williams–Landel–Ferry (WLF) equation (see, e.g. Ferry [4]). The WLF approach, originally empirical but usually analysed theoretically in terms of free volume changes, leads to temperature-dependent activation energies and predicts that molecular motion will become "frozen" at temperatures about 50° C below T_g, which might be seen as an "effective absolute zero". In comparison to this more detailed approach, the two-mode model will thus predict too rapid a rate of recovery in the glass. The important positive feature of the two-component approach is that the resolution of deformation into an orientational and a non-orientational component, subject to different rate effects (however we choose to formulate the rate dependence), leads in general to different relaxation rates for molecular orientation and overall strain. It is this facility which is required if the experimentally observed relative behaviour of orientation and strain is to be successfully described.

We have of course neglected viscous flow effects in systems which lack a permanent cross-link network. However, any such genuinely irrecoverable component of deformation is easily enough visualized in terms of the "pulling-out" of some of the chain tangles and chain ends; it will be most significant for shorter chains.

7. Relaxation and annealing effects

Stress relaxation experiments are perhaps most commonly associated with creep studies, but the work discussed in Part 1 suggests that the modelling of relaxation behaviour may be of use in considering deformation mechanisms. It will be recalled that one of the original stimuli for the two-component approach to deformation was the differing behaviour of orientation and of overall strain when comparing deformation above and below T_g, or when considering relaxation.

7.1. Modelling stress relaxation

To apply the model to stress relaxation, the stepwise computation is performed up to some specified value of q. Stress relaxation is then modelled by setting Δt to a constant for subsequent steps and reducing q at each step such that the extension ratio λ remains constant (to within a specified accuracy, typically 0.1%): the appropriate reduction in q is found by an iterative method involving a "binary division" procedure. The decrease of q, and concomitantly of orientation, is monitored as a function of time, so that the situation is to be likened to a stress relaxation experiment at constant nominal strain.

A note of caution is again required: under conditions of stress relaxation we should anticipate greater inadequacies in the two-mode approach as so far developed, due to coupling between the deformation modes, than under conditions of simple loading. As indicated in Part 1, this will be a consequence of the differing time sensitivity of the deformation modes: essentially, the two modes will "try to relax" at rates which may be in a different ratio from the rates at which they, cooperatively, gave rise to the original deformation.

With a rate effect applied only to the extensional mode the modelling is straightforward. Fig. 12 shows the "decay" of stress towards a finite asymptote during relaxation. This finite stress level will correspond to the "fast model" stress appropriate to the strain. The "loading" stress–strain plot for Curves A to C is Curve A of Fig. 8: the fact that Curves A, B, C start from similar values of the nominal stress parameter Q is fortuitous but convenient. With a less severe rate effect (Curve D) the possible degree of relaxation is reduced.

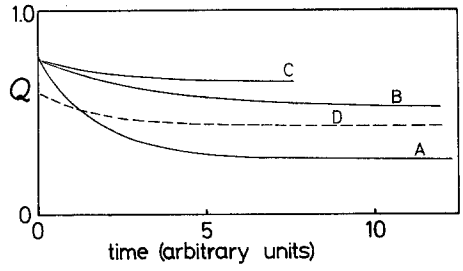

Figure 12 Modelling stress relaxation at constant strain. Aspect ratio 3, $K = 3$, rate effect on extensional mode only. $\Delta\lambda/\Delta t = 0.1$ during loading. (A) $C_e = 0.125$, loaded to $q = 1.0$ and relaxed; (B) $C_e = 0.125$, loaded to $q = 1.5$ and relaxed; (C) $C_e = 0.125$, loaded to $q = 2.0$ and relaxed; (D) $C_e = 0.25$, loaded to $q = 1.0$ and relaxed.

The next step – the quantitative application of the "stress relaxation" procedure to the more complex case where both deformation modes are subject to rate effects – is attended by computational difficulties: it will not be dealt with further in the present paper.

7.2. Modelling annealing

The behaviour of the model corresponding to annealing at low temperatures (e.g. below T_g) may be examined by loading as before to a specified value of q and then removing the load instantaneously – a situation analogous to a "load, quench, unload" experiment. The step time Δt is again set to a constant, and the decay of strain and of orientation monitored. We can specify different rate constants during loading and during "annealing": the two rate constants should remain in a constant ratio (presumably a material property), but their absolute values will depend on temperature. Initial deformation in the rubbery state (no rate effects) is modelled by setting C_0 and C_e to be very large during loading.

It is convenient to plot this decay in a form similar to that used by Kahar *et al.* [5] in displaying their results for PMMA annealed slightly above T_g (at 116.5° C). We determine $\langle P_2\rangle/\langle P_2\rangle_0$, where $\langle P_2\rangle$ is measured as a function of time and the suffix zero denotes the value at the start of the "anneal", and plot this ratio against the corresponding fractional strain (we use the fractional true strain ϵ_t/ϵ_{t0}). Both quantities decay from 1 towards 0 with time (Fig. 13). The orientation parameter $\langle P_2\rangle$ decays rather more rapidly than

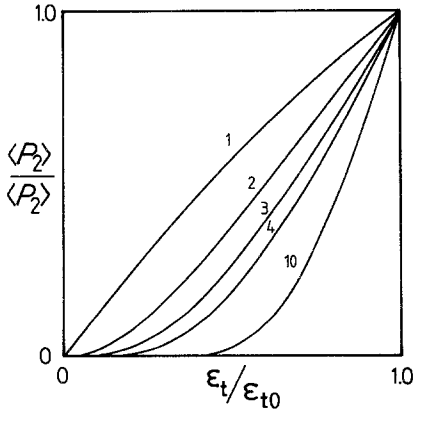

Figure 13 Fractional orientation plotted against fractional strain during "annealing". The model is "loaded" to $q = 2$ and allowed to "recover" with C_0/C_e taking the values indicated (aspect ratio 3, $K = 3$).

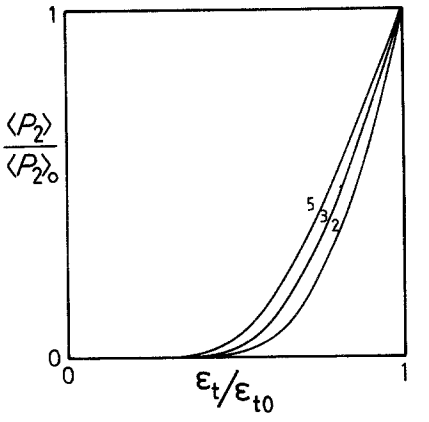

Figure 14 Fractional orientation plotted against fractional strain during "annealing" with $C_0/C_e = 10$, $K = 3$. Number denotes aspect ratio.

overall strain, even if equal rate constants are applied to the two deformation modes; as we increase the ratio C_0/C_e (i.e. make the extensional rate effect relatively more severe) the curvature of the plot, not surprisingly, increases, taking a shape comparable to the experimental behaviour recorded by Kahar *et al.* Kahar *et al.* worked at 116.5° C, i.e. just above T_g, but in a regime where rate effects are of sufficient importance to make recovery slow enough to be followed quantitatively.

There are several parameters which might affect the "decay curve". The curvature is increased for units of smaller aspect ratio (Fig. 14), but dependence on K is extremely slight. Dependence on the extent of the original deformation (i.e. the as-deformed strain) is also slight, and the same curve is generated whether the model is subjected to the rate effects during loading (i.e. as well as during recovery) or not. For a fixed aspect ratio, then, the shape of the curve is essentially controlled by the ratio of the two rate constants during "annealing". Their absolute values are immaterial: in terms of real polymers, this indicates that the "decay curve" will be independent of the original deformation temperature (assuming that temperature will not affect the ratio C_0/C_e, but only their absolute values, that is, merely the speed at which the specimen "slides down the decay curve"). These features are again in accordance with the observations of Kahar *et al.*, who found that samples of PMMA extruded at 50, 90 and 110° C all followed the same curve. Over a wide temperature range we might nevertheless anticipate some difference, if the effects of

any "coupling" between the two deformation modes is temperature dependent. Any coupling might be more effective where the longer-range extensional component predominates, thus interfering with recovery. This could help to account for the lesser degree of recovery in PMMA deformed as a rubber and quenched, than in a sample deformed as a glass.

More qualitatively, the model also accords with indications from the work of Brady and Yeh [6, 7] that orientation decays more rapidly than overall strain on annealing slightly below T_g. This work, covering polystyrene and polycarbonate as well as poly(methyl methacrylate), has been discussed in Part 1.

8. More general effects of temperature

The mechanical behaviour of a non-crystalline polymer is most dramatically affected by changes in temperature when the material passes through its glass transition. At temperatures below the transition, the deformation is characterized by pronounced sensitivity to strain rate and therefore to time.

However, the deformation behaviour is temperature sensitive quite apart from changes associated with the glass transition. The sensitivity is to some extent less strong above T_g but it is nevertheless significant. In more conventional approaches to rubber-like deformation, the simple proportionality of the "rubber modulus" NkT to temperature is insufficient to describe the temperature variation of mechanical behaviour alone, and temperature effects are dealt with in terms of variations in the size of the statistical equivalent random link and, in some systems, the effect of temperature on strain-induced crystallization.

In considering the two-mode model developed in Part 2, three principal effects of temperature may be anticipated. Firstly, and most manageably, we have the conversion between the dimensionless parameter q and true stress σ ($q = v\sigma/kT$) so that, other things being equal, the conversion factor σ/q will be proportional to absolute temperature.

Secondly, we have the question of any temperature dependence of the volume per mobile unit v. It is possible that some large change in v may be associated with the glass transition; but it is also possible that v will vary with temperature well away from T_g. We might compare this to the temperature dependence of the apparent size of the statistical random link in conventional rubber elasticity theory. It may be, for example, with increased thermal activation, that sections of chain undergo deformation independently rather than as "bundles". Associated with any such change in v would be a possible change in the effective unit aspect ratio. Changes in v will affect only the "scaling" on the stress axis, so that the conversion factor σ/q will no longer be exactly proportional to absolute temperature. Concomitant changes in unit aspect ratio will, in contrast, affect the shape of the nominal stress–strain plot itself, independently of scaling. We may speculate that a continuous variation of aspect ratio would be less plausible than step changes near specific temperatures, i.e. as chain segments move from cooperative deformation ("bundles") to independent motion.

Thirdly, it may be anticipated that the "fractional constraint" $1/K$ may be temperature dependent. We might expect that the mean constraint would tend to decline as temperature, and hence thermal activation, increases, and we can liken this to the expectation from a more conventional viewpoint that with increased thermal activation and chain motion some of the mechanical interlinking (steric effects and chain "tangles", though not topological entanglements) will become less effective.

In the finite-rate modification of the model, we have the additional effect of temperature upon the rate sensitivity itself. Firstly, it will be recalled that the factor F in Equation 9, and hence C_e, contains a term $\exp(-\Delta E/kT)$, related to an "activation barrier"; and secondly, the pre-exponential term may itself be temperature dependent. Similar considerations can be applied to C_0 in the more empirical Equation 13. Further, the nature of possible "coupling effects" between the two deformation modes may be expected to show a temperature sensitivity. The breakdown of steric or other interactions (or however we physically picture coupling) will presumably be thermally activated to some extent, and a small change in the efficiency of these interactions might have disproportionately great repercussions regarding, for example, the degree to which recovery of strain and orientation after deformation is prevented.

While these speculative comments indicate that the possible effects of temperature on the characteristic nominal stress–strain plot are rather complex, they also highlight the value of following trends in mechanical behaviour using measurements

of orientation as well as stress–strain measurements. This is particularly so since the $\langle P_{2n} \rangle$–strain plots will be unaffected by scaling effects in the conversion from dimensionless units of q to those of stress; these plots will hence reflect only changes in the two central parameters themselves, and the associated trends may then be more clearly seen.

9. Experimental data viewed in the light of the model

Comparison of the two-mode model with experimental data relating to polymer glasses must be approached a little more tentatively than for the rubbery regime: this follows both from the less fully developed nature of the finite-rate model, and from the overall picture presented by the literature – a less rationalized and apparently more complex one than is the case for "classical" rubbers. The finite-rate modification of the basic two-mode model necessarily involves an additional element of uncertainty compared to the fast model, in the question of the values to be assigned to the rate constants. If we are content to consider arbitrary units of strain rate, the rate effects reduce to effectively one important parameter, the ratio C_0/C_e.

9.1. Factors affecting the shape of the stress–strain curve

The shape of the stress–strain curve for a polymer glass is highly sensitive to experimental geometry and conditions; in particular, whether the technique is "hard" (as in a screw-driven testing machine) or "soft" (as in a dead-loading system, imposing a monotonically increasing load and hence preventing any yield drop being recorded). In practice, most mechanical tests fall somewhere between the "hard" and "soft" extremes.

The model, as indicated above, implies a monotonically increasing true stress, which would be something difficult to produce experimentally in a uniaxial geometry. Nevertheless, the general trends exhibited by the model as the effective strain rate is increased are in accordance with experiment. They include the steeper initial region, the increasing "threshold stress" analogous (at least qualitatively) to yield, and the subsequent fall in nominal stress followed by a further increase as the limiting strain is approached.

We cannot deal quantitatively with the initial modulus, since experimental moduli will include an unknown contribution of an "energy-elastic" nature; it is also because of this that the "threshold" effect predicted by the model is sharper than anything which would be seen by experiment.

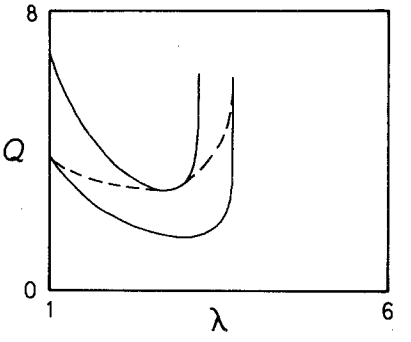

Figure 15 Effect of necking on the load drop. The two solid curves differ in strain rate by a factor of 4. Dashed curve: expected curve after allowing for necking (schematic).

In practice, the presence of a yield drop will be associated with the localization of deformation in a neck in a uniaxial test (or a shear band in, for example, a plane strain test). If a constant strain rate is imposed on the specimen as a whole, the strain rate within the neck will be higher, by a proportion dependent on the "draw ratio" and the ratio of neck length to gauge length. To imitate such a localization of deformation in the model, one would have to increase the effective strain rate accordingly once the threshold stress is attained. Such a modification would have the effect of "filling up the load drop", as illustrated (very schematically) in Fig. 15.

The effect of a "distribution of constraint", discussed above, will also be significant here. It will tend to "smear out" the approach to the limiting strain: indeed, the limiting strain will be less well defined. Fig. 16 is an attempt to depict this, again very schematically. Allowance for these two

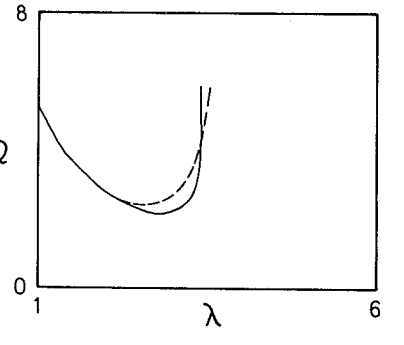

Figure 16 Effect of a distribution of constraint. Solid curve: as computed. Dashed curve: expected curve after allowing for distribution (schematic).

factors would tend to bring the predicted stress–strain curves nearer to those typically observed experimentally.

9.2. The absolute magnitude of the rate constants

It is instructive to estimate the magnitude of the "activation barrier" associated with the behaviour modelled above. We consider for simplicity only the stronger, extensional rate effect, controlled by the parameter C_e. The strain rate, in the arbitrary units of Figs. 9, 10 and 11, is given by

$$\text{rate} = 40(\Delta\lambda/\Delta t)/C_e \qquad (15)$$

If t is in seconds and a nominal strain rate of 10^{-3} sec^{-1} is chosen, the finite-rate curves of Fig. 9 require C_e in the range 1.0×10^{-4} to 1.6×10^{-3}.

We recall that C_e is defined as $f \exp(\Delta E/kT)$, with ΔE the height of the activation barrier. If the frequency factor f is set to the Debye frequency f_d ($\sim 10^{13}$ sec^{-1}) we write

$$\Delta E/kT = \ln(f_d/C_e) \qquad (16)$$

and the above values of C_e then give ΔE in the range 36.4 to 39.1 kT. The logarithm means that large changes in f/C_e will give only small changes in ΔE. Escaig and Lefebvre [8], in their treatment of activated plasticity, suggest that the Debye frequency is an upper bound to the effective vibration frequency, since it corresponds to uncorrelated segment motion, and that a better estimate is obtained by dividing f_d by the number of segments involved in the activation process: they take the value $0.1f_d$. This would alter the range determined above to between 34.1 and 36.8 kT.

This estimate of ΔE is rough, but it is of a reasonable order of magnitude. It may be compared to the activation barrier for yielding of order $50kT$ (for a strain rate of 10^{-3} sec^{-1}) used by Bowden and Raha [9], or to the activation barrier of "about $20kT$" quoted by Escaig and Lefebvre [8].

9.3. Rate effects and the orientation behaviour of PMMA

The development of orientation with strain and with stress has been discussed above. Where data are obtained by a quench–unload method, we know [10] that points well below T_g lie roughly on a common $\langle P_2 \rangle$ against strain line. The $\langle P_2 \rangle$–strain plot for the model is independent of the conversion factor from q to stress (i.e. of v), and so its primary temperature dependence will come from two factors: firstly any increase in constraint with decreasing temperature; and secondly the reduction in C_o and C_e with decreasing temperature (i.e. the rate effects become more severe). These factors would oppose one another. The temperature dependence of the $\langle P_2 \rangle$–strain plot for the fast model was tentatively attributed above to the former: however, it is much less easy to visualize changes in such a molecular parameter in the glassy state, where the absence of long range mobility will prevent the constraint being reduced, as suggested earlier for rubbers, by mechanisms such as the "pulling-out" of chain tangles.

The effect of increasing the severity of the rate effects depends on the ratio C_o/C_e. Applying a rate dependence to each mode, with a difference in the rate constants of one order of magnitude, leads to the trends already illustrated in Fig. 10, with the parameter values suggested in Part 1 for PMMA. The behaviour shown suggests a tentative rationalization of reported data. Firstly, it predicts the rise in SNOCP as the system is cooled below T_g – a rise which is appreciable, though not comparable to the change in modulus. Secondly, it indicates how orientation–strain curves at various temperatures below T_g may approximately superimpose, at least at low degrees of orientation, as found by Pick *et al.* [10]. Thirdly, it may cast light on why the superimposition observation was not made by other workers (e.g. [10, 11]). In addition to some important differences in experimental technique, we now have the possibility that with somewhat fortuitous choices of material, temperature and strain rate, the orientation–strain data of Pick below T_g fell nearer to the "maximum-slope" curve of Fig. 10 than those of other workers.

The ratio $C_o/C_e = 10$ predicts a maximum SNOCP higher by about a factor of 6 than the fast model value. Pick's data are roughly in accordance with this, though the scatter precludes a precise comparison. To confirm the predicted trends would require the determination of orientation–strain curves at lower temperatures and/or higher strain rates than those of Pick *et al.* This would be experimentally difficult because of the tendency to brittle fracture under such conditions, and in birefringence experiments the high modulus may cause stress birefringence to swamp birefringence due to orientation.

Because of the higher stresses involved, the development of birefringence in the glass will be

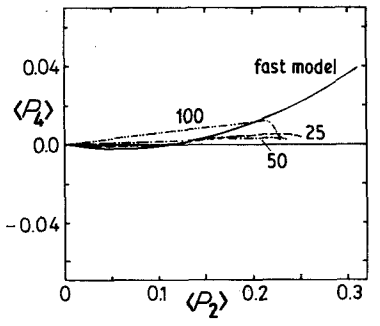

Figure 17 $\langle P_4(\cos\phi)\rangle$ plotted against $\langle P_2(\cos\phi)\rangle$ for the finite-rate model. Aspect ratio 1.46, $K = 4.5$, $C_o/C_e = 10$. Number denotes strain rate (arbitrary units).

complicated by stress birefringence effects to a greater degree than in the rubber. This will be particularly significant for measurements made under load, though even after unloading some of the stress contribution may not be able to recover rapidly before the birefringence is measured.

9.4. $\langle P_4(\cos\phi)\rangle$

Values of $\langle P_4\rangle$ for temperatures below T_g, like those for the rubbery regime, remain low at all accessible strains (except for some determined by methods such as laser-Raman spectroscopy, where results must be treated with some caution owing to difficulties in the analysis of the scattering data, due to uncertainty about line assignment and the nature of the Raman tensor). The available WAXS data [10 12] would suggest only a gradual change on passing through T_g, with the tendency towards negative $\langle P_4\rangle$ becoming a little clearer at lower temperatures. The analysis of orientational deformation below T_g in terms of the pseudo-affine scheme predicts that $\langle P_4\rangle$ will, except at very low strains, increase rapidly with strain so as to be comparable in magnitude with $\langle P_2\rangle$ at strains above perhaps $\lambda = 2$. This is in sharp contrast to the affine prediction above T_g, and conflicts with the experimental indications referred to above.

The two-mode model, by contrast, predicts low $\langle P_4\rangle$ even when severe rate effects are applied. The application of a rate effect to each deformation mode has the effect of straightening out the $\langle P_4\rangle$ against $\langle P_2\rangle$ plot (Fig. 17). The uncertainty in the computed $\langle P_4\rangle$ increases rapidly as the orientational rate effect becomes more severe, and at rates greater than those indicated in Fig. 17 too few points are computed in the appropriate range of $\langle P_2\rangle$ (because of the high $d\langle P_2\rangle/dq$) to allow a useful plot to be made. Nevertheless, one may draw the qualitative conclusion that the finite-rate model does not predict the sharp upward curvature typical of the pseudo-affine deformation scheme: the fast model case will represent the most pronounced curvature on the $\langle P_4\rangle$ against $\langle P_2\rangle$ plot obtainable from the two-mode model.

Data for $T < T_g$ (as in Mitchell *et al.* [12]) are shown in Fig. 18. Neither the pseudo-affine nor the two-mode model affords a good fit, with the exception of the data for 100° C (just below T_g) which are fairly well described by the two-mode model in the absence of rate effects. One might tentatively conclude that typical two-mode predictions lie close to the data than do the affine and pseudo-affine curves, though to predict the magnitude of the negative $\langle P_4\rangle$ would require aspect ratios larger than the 1.46 suggested for rubbery PMMA. However, firm conclusions would have to await more precise $\langle P_4\rangle$ data than have so far been obtained.

9.5. Annealing and relaxation effects

The basic philosophy behind the two-mode model gives preferential recovery of the orientational component of strain, and hence leads quite natur-

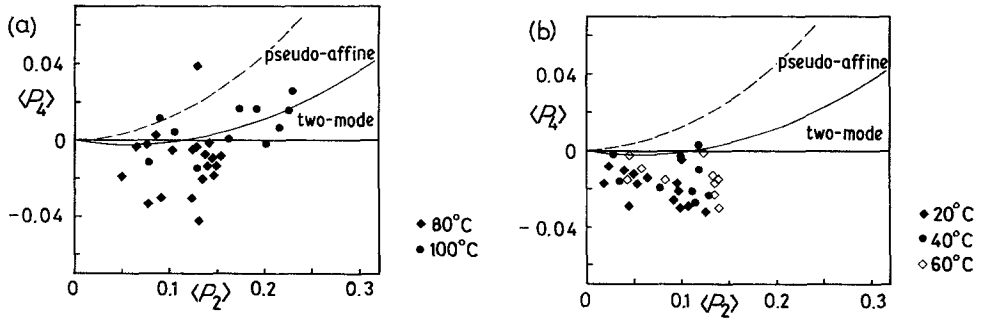

Figure 18 $\langle P_4(\cos\phi)\rangle$ plotted against $\langle P_2(\cos\phi)\rangle$ for PMMA deformed in plain strain (data from Mitchell *et al.* [12]). Solid curve: two-mode model, aspect ratio 1.46 (fast model). Dashed line: pseudo-affine.

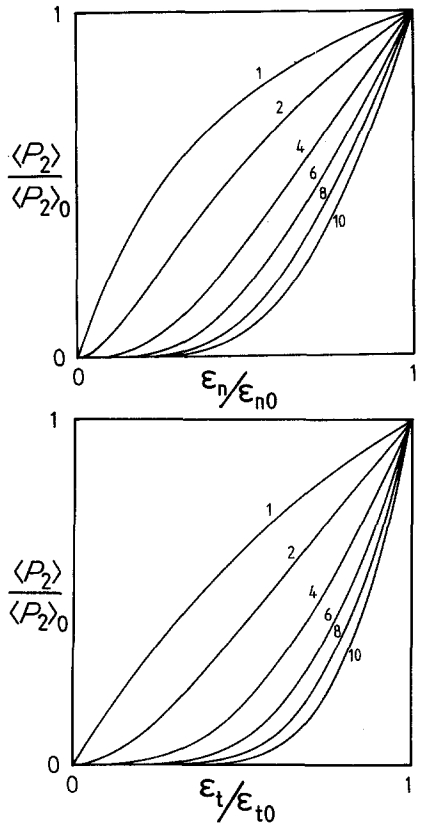

Figure 19 Orientation and strain recovery: aspect ratio 1.46, $K = 4.5$, originally loaded to $q = 2$ (giving $\langle P_2\rangle = \langle P_2\rangle_0$, strain ϵ_{n0} or ϵ_{t0}). Number denotes ratio C_o/C_e. (a) nominal strain ϵ_n; (b) true strain ϵ_t.

ally to the form of recovery behaviour observed quantitatively by Kahar *et al.* [5] and somewhat more qualitatively by Brady and Yeh [6, 7]. The curvature of the predicted "decay curve" increases with the ratio C_o/C_e, and by comparing it with the experimental curve recorded by Kahar *et al.* one can derive a rough estimate of a reasonable value of this ratio for PMMA.

The comparison (Fig. 19) indicates that a ratio of order 7:1 would be appropriate for prediction of the general trends in the orientation–strain behaviour of PMMA* (Fig. 20) – not far from the arbitrary choice of one order of magnitude made above. The curves cannot be expected to match precisely: we have already discussed the importance of coupling between the deformation modes, and different techniques of orientation determination may give different rates of orientation recovery [6, 7]. Nevertheless, with this rough estimate of C_o/C_e we move a little nearer to quanti-

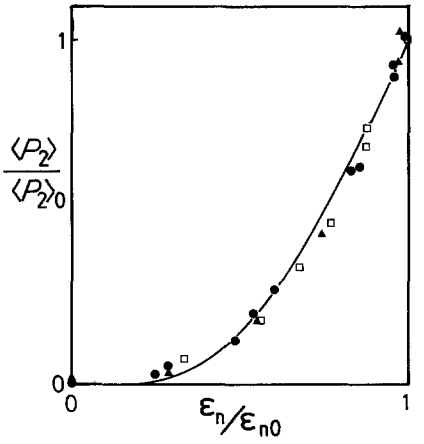

Figure 20 Orientation and strain recovery: as Fig. 19, with $C_o/C_e = 7$. Data: Kahar *et al.* [5]. Deformation temperature: • 50° C, ▲ 90° C, □ 100° C.

tative modelling of PMMA in the glassy state; or more strictly, at temperatures which are not so far above T_g that rate effects may be neglected.

The further observations of Kahar *et al.* in regard to the finite limiting shrinkage stress can also be related to the two-mode model. The model would predict that at long times the shrinkage stress will tend to a limit which is a function only of strain, independent of the temperature and rate effects applicable to the original deformation. This accords with the observation that specimens deformed at different temperatures but to the same strain exhibited the same limiting shrinkage stress, while those deformed to the same birefringence but at different temperatures, giving different strains, did not. The limit will simply be the "fast model" stress appropriate to the strain in question, as discussed above. The initial peak shrinkage stress, which varied with as-deformed birefringence, may be a reflection of internal stresses which have been unable to recover. A greater stress is required to deform a specimen at lower temperature (for a fixed strain and strain rate) and we may expect a higher peak stress, other things being equal, when the specimen is heated to allow shrinkage to occur. The higher as-deformed birefringence could be interpreted in the light of the model too: from Fig. 10 we see that over at least part of the range shown, a lower temperature (i.e. more severe rate effects) will lead to greater orientation at intermediate strains. The extrusion technique allowed strains up to $\lambda = 2$ (100%) to be attained. Part of the birefringence

*In making this rough estimate the slight dependence of the curve on the extent of the original deformation is neglected.

after extrusion recorded by Kahar *et al.* may, however, be attributable to the stress contribution (rather than to the "orientation" contribution); this would be enhanced at lower temperatures because of the higher stress associated with a given strain.

10. Summary

Rate dependence is introduced into the two-mode model in a deliberately simplified form, in order to see what features of deformation can at least qualitatively be described with a minimal number of additional adjustable parameters. In practice they will represent – rather like the constraint concept introduced in Part 1 – overall parameters which may be seen as describing the properties of the material, or of the assemblage of orienting units, averaged over regions large compared to chain spacings. Such an approach bears some comparison with one of the underlying ideas of "tube models": that a polymer chain is so long and interacts with so many other molecules, that its environment may be treated as a continuum, with properties characteristic of the material in bulk. While the rate constants might possibly be seen in relation to some single dominant activated process affecting a particular deformation mode, the applicability of the model does not directly require that this should be the case.

The introduction of rate dependences into the two-mode model has succeeded in describing at least qualitatively some of the trends to be expected when going from the rubbery to the glassy regime. These features include the drastic increase in the initial slope of the stress–strain curve, and the subsequent drop in nominal stress, which becomes more pronounced with increasing severity of the rate effect (i.e. as the values of the rate constants are decreased, or as the imposed strain rate is increased). With a suitable choice of C_o/C_e, the ratio of the rate constants associated with the two modes, the increased initial slope of the $\langle P_2 \rangle$ against strain plot may also be modelled: for PMMA, a ratio 7 : 1 seems to be appropriate.

Where a severe rate effect is imposed, with rate constants applied to both deformation modes and the effective strain rate held constant, the model predicts behaviour which is very reminiscent of yield – even though no specific yield process has been introduced. There remains, however, some doubt over the magnitude of the "threshold" level of the true stress parameter q in relation to the experimental yield stress, as a function of strain rate. The constant nominal strain rate condition also reduces the effective maximum strain of the system as the severity of the rate effect is increased.

The predicted levelling-off of the $\langle P_2 \rangle$–strain plot, where the extensional rate effect is relatively severe, suggests that experimental birefringence–strain plots may give a misleading indication as to the birefringence corresponding to $\langle P_2 \rangle = 1$: a plot which does not extend close to the limiting strain will appear to be approaching an asymptote which does not coincide with $\langle P_2 \rangle = 1$. As in the "fast model", $\langle P_4 \rangle$ remains low: in the constant strain rate model this is true even up to the effective limiting strain.

The principle of resolving deformation into orientational and non-orientational components allows the description of stress relaxation and annealing behaviour, including the experimental observation that orientation is more susceptible to recovery than is overall strain. Full quantitative modelling of stress relaxation would require much further work, but would be worthwhile though costly in computer time.

The model has not taken into account the "energy-elastic" contribution, analogous to that involved in crystal deformation – a contribution which will be more significant in the glassy than in the rubbery regime, on account of the higher stresses involved, and which will be associated with the non-isovolumetric nature of glassy deformation. While the omission of this contribution is not expected to affect the overall shape of the stress–strain curve very much, it will have an important effect on the initial modulus.

As one would have anticipated, the effect of coupling between the deformation modes appears to be more significant in the glassy than in the rubbery state. Though the two-component approach makes the assumption that the modes may be taken as independent to a first approximation, the secondary effect of interactions between them – particularly under relaxation or annealing conditions – should always be borne in mind.

Thus, the profound differences both in the stress–strain and in the orientation–strain relationships characteristic of the rubbery and glassy states can be accounted for by the two-mode deformation model. A semi-quantitative prediction of the mechanical and orientational behaviour of the glass can be obtained by the simple application of

a rate constant to each of the two deformation components of the model. At the same time, one is able to explain annealing effects in deformed glasses where orientation is seen to recover more readily than strain.

Acknowledgements

In preparing this series of papers the authors have been able to draw on recent developments of orientation measurement in which Dr G. R. Mitchell has played a key role. They are grateful for his interest and involvement in the work, and also wish to thank Professor M. Gordon for illuminating discussions. Financial support from the Science and Engineering Research Council is acknowledged with thanks, as is the provision of laboratory facilities by Professor R. W. K. Honeycombe and of computing resources by the University of Cambridge Computing Service.

References

1. D. J. BROWN and A. H. WINDLE, *J. Mater. Sci.* 19 (1984) 2013.
2. H. EYRING, *J. Chem. Phys.* 4 (1936) 283.
3. D. J. BROWN and A. H. WINDLE, *J. Mater. Sci.* 19 (1984) 1997.
4. J. D. FERRY, "Viscoelastic Properties of Polymers", 2nd edn, (Wiley, New York and London, 1970).
5. N. KAHAR, R. A. DUCKETT and I. M. WARD, *Polymer* 19 (1978) 136.
6. T. E. BRADY and G. S. Y. YEH, *J. Polym. Sci., Part B* 10 (1972) 731.
7. *Idem, J. Macromol. Sci. Phys.* B7 (1973) 243.
8. B. ESCAIG and J. M. LeFEBVRE, *Rev. Phys. Appl.* 13 (1978) 285.
9. P. B. BOWDEN and S. RAHA, *Phil. Mag.* 29 (1974) 149.
10. M. PICK, R. LOVELL and A. H. WINDLE, *Polymer* 13 (1980) 1017.
11. S. RAHA and P. B. BOWDEN, *ibid.* 13 (1972) 174.
12. G. R. MITCHELL, M. PICK and A. H. WINDLE, *Polymer Commun.* 24 (1983) 16.

Received 7 September
and accepted 22 September 1983